Analysis of long-term rainfall trends and change point in Bandama Basin, Côte d'Ivoire

N'Guessan Kouamé Emmanuel Abo and Gneneyougo Emile Soro

Laboratoire Géosciences et Environnement, Université Nangui Abrogoua, Abidjan, Côte d'Ivoire

ABSTRACT: The objective of this study is to analyses long-term trends and rainfall breaks in the Bandama River catchment. To achieve this objective, the study used data from nineteen (19) rainfall stations from 1950 - 2020. The methodology adopted was based on the Mann Kendall (classical and modified), Krusal Wallis and Cumulative Deviation statistical tests to detect and analyses significant changes in the rainfall series. The results show that 58% of the stations show a significant downward trend at the 5% risk without taking into account the Hurst effect, while with the Hurst effect only 32% of the stations show significant downward trends at the 5% risk. The breaks detected in this study oscillate around 1970 with a deficit ranging from -6% to 23 %. Furthermore, the Moran Index (MI) revealed a spatial dependence in the rainfall series of the catchment.

KEYWORDS: West Africa, Bandama, Climate change, Hurst phenomenon, Statistical test.

1 INTRODUCTION

West Africa is a region that is particularly vulnerable to climate change. The vulnerability of sub-Saharan Africa to the effects of climate variability and change is one of the issues most discussed by the scientific community, institutions and the media. Because of its low capacity to adapt and the high sensitivity of its socio-economic systems, this part of the world is one of the most vulnerable regions to climate change [1]. Like most countries in sub-Saharan Africa, Côte d'Ivoire is also vulnerable to the effects of this phenomenon. Long-term climate change linked to changes in rainfall patterns and rainfall variability is very likely to increase the frequency of droughts and floods in this country. Côte d'Ivoire has a strong relationship with the climate because of its economy based on rain-fed agriculture and its heavy dependence on the flow of rivers for the production of hydroelectricity. This climatic variability manifested itself in Côte d'Ivoire towards the end of the 1960s and early 1990s in a downward trend in rainfall ([2], [3], [4], [5]). It first affected the north, then gradually spread to the center and finally to the coast [6]. These rainfall anomalies have had an exceptional impact on the country's northern and central regions. In Côte d'Ivoire, there are several studies on climate variability and rainfall trends over the period 1960-2000, for example ([7], [8], [9]), but few ([10], [11], [12]) have looked at climate variability in the early years of the 21st century. While temperature increases are a certainty, precipitation trends are much more mixed, as they are subject to strong spatial-temporal variability. The aim of this study is to examine the long-term evolution of annual rainfall in the Bandama catchment, one of the basins subject to anthropogenic pressures and whose water resources are much in demand for multiple uses. Indeed, the detection of trends and abrupt changes in its rainfall series are fundamental questions in understanding the response of the hydrological environment to the effects of climate change, particularly in terms of freshwater availability.

2 DATA AND METHODS

2.1 OVERVIEW OF THE STUDY AREA

The geographical location of the study area is shown in Figure 1. The Bandama river basin is located in Côte d'Ivoire. The river rises in the north of Côte d'Ivoire between the towns of Korhogo and Boundiali. Its catchment area covers 97,000 km2 and is 1,050 km long. The Bandama basin extends over three climatic regimes. Its northern part is characterized by a dry subtropical climate (between 1000 mm and 1700 mm). This zone has a unimodal rainfall distribution or regime, with distinct

---

wet (rainy) and dry seasons. The central (equatorial climate) and southern (humid equatorial climate) parts of the basin are characterized by two rainy seasons. In the equatorial climate, annual rainfall exceeds 1,500 mm. The amount of rainfall is higher in the humid equatorial climate, with an annual average of 1800 mm. Vegetation cover in the Bandama catchment area varies from north (savannah) to south (forest). The topography of the Bandama catchment is gentle, with a maximum elevation of 809 m above sea level.
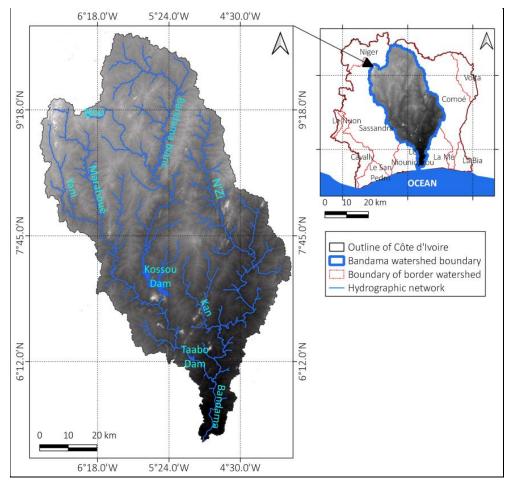

Fig. 1.   Geographical location of the Bandama River watershed

2.2   DATA

The climatic data was made available by the National Meteorological Department of Côte d'Ivoire (SODEXAM). The data consists of annual rainfall for the period 1950-2020. The gaps detected were filled using the Regional Vector method. The stations were chosen to ensure good spatial coverage of the different climatic zones in the Bandama basin (Figure 2). Meteorological stations located outside the catchment were used because the climatic variables measured at these stations influence the flows in the catchment.
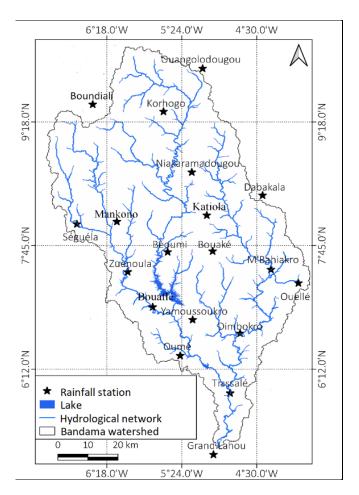
Fig. 2.   Spatial distribution of the rain gauge stations

2.3   METHODS

2.3.1   DETECTION OF LONG-TERM TRENDS

2.3.1.1   MANN KENDALL TEST WITHOUT TAKING AUTOCORRELATION INTO ACCOUNT

The classic Mann-Kendall test is used to check whether there is a trend in time series data. This non-parametric test is robust to the influence of extremes and can be applied to biased variables [13]. More specifically, this non-parametric trend test is the result of an improvement on the test first studied by [14], then taken up by [15] and finally optimised by [16], [17] and [18].

The Mann-Kendall test is based on the sign of the difference between the ranks of a time series. Let X = (x1, x2,...xn) be a time series, and the Mann-Kendall statistic is given by:

$$a_{ij} = sign(x_j - x_i) = sign(R_j - R_i) = \begin{cases} 1 \text{ si } x_j > x_i \\ 0 \text{ si } x_j = x_i \\ -1 \text{ si } x_j < x_i \end{cases}$$

And R_j, R_i are respectively the ranks of observations x1 and x2 in the series. Under the assumption that the data are independent and identically distributed, the mean and variance of the test statistic S above are given by [15]:

$$E(S) = 0$$

$$Var(S) = \frac{n(n-1)(2n+5)}{18}$$

Where n is the size of the series. The existence of equal observations in the series leads to a reduction in the variance of S, which becomes:

$$Var(S) = \frac{n(n-1)(2n+5)}{18} - \sum_{j=1}^{m} t_j \, (t_j-1) \, (2t_j+5) \, /18$$

Where m is the number of groups of equal observations and tj is the number of equal observations in group j. We can normalise the test statistic and obtain a new test statistic u:

$$U = \begin{cases} \dfrac{(S-1)}{\sqrt{V_0 \, (S)}} & \text{si } S>0 \\ 0 & \text{si } S=0 \\ \dfrac{(S+1)}{\sqrt{V_0 \, (S)}} & \text{si } S>0 \end{cases}$$

Where the subtraction or addition of the unit corresponds to a continuity correction.

The test statistic u is asymptotically Gaussian. The significance of the trend can therefore be assessed under hypothesis H_0 by comparing the p-value=P (Z>u) (for a one-tailed test) or p-value=2P (Z>|u|) (for a two-tailed test) and the confidence level α. If p-value <α we reject H_0 at risk α, if not we do not reject H_0.

2.3.1.2 TEST DE MANN KENDALL AVEC PRISE EN COMPTE DE L'AUTOCORRELATION

This is a complementary approach to the classic Mann Kendall test, which takes into account the phenomenon of autocorrelation. This test can only be applied if the chronicle has forty (40) or more analyses [19]. Its principle is based on a modification of the Mann-Kendall S test rather than modifying the data themselves:

$$Var_\rho(S) = \gamma . Var_{\rho=0}(S)$$

Where γ is a correction factor applied to the variance [20]. The mean and variance of the Mann-Kendall (S) statistic under the assumption of long-term persistence (LTP) are given by [13]:

$$E\,(S) = 0$$

$$Var\,(S) = \sum_{i=1}^{n-1} \sum_{j=i+1}^{n} \sum_{k=1}^{n-1} \sum_{l=k+1}^{n} \frac{2}{\pi} \sin^{-1} \left(\frac{\rho_{jl} - \rho_{il} - \rho_{jk} + \rho_{ik}}{\sqrt{(2-2\rho_{ij})\,(2-2\rho_{kl})}} \right)$$

Where $\rho_{ij} = \rho\,(j-i)$ i =1: n are the autocorrelation coefficients.

The significance level chosen for autocorrelation is 5%.In practice, autocorrelation coefficients must be calculated using an estimate of the Hurst coefficient in the autocorrelation formula ρ (h).

$$\rho(h) = \frac{1}{2} \left[|h+1|2H - 2|h|2H + |h-1|2H \right]$$

With h ≥ 0; H is the Hurst parameter.

Hamed proposes to use a maximum likelihood (ML) approach derived from that proposed by [21]. The main steps are as follows:

First, we need to remove the trend on the data using the non-parametric trend estimator of [22] which is given by:

$$S_o = \text{médiane} \left(\frac{x_j - x_i}{j-1} \right)_{(i<j)}$$

Equivalent normal variables Zt are then obtained by a "normal score" transformation:

$$Z_t = \Phi^{-1}\left(\frac{R_t}{n+1}\right)$$

Where Rt is the rank of the observation whose trend has been removed, n the number of observations and φ-1 (.) is the inverse of the distribution function of a reduced centered normal law.

Finally, the Hurst coefficient can be estimated by maximizing the log-likelihood function:

$$\text{Log } L\,(H) = -\frac{1}{2}\log|C_n\,(H)| - \frac{Z^T\,[C_n\,(H)\,]^{-1}}{2\gamma 0}Z$$

Où $Z = (z_1, z_2,..., z_n)$, $\gamma 0$ = var (Z) et [C_n (H)] = [ρ (j - i)], i = 1: j = 1: n

The estimate of H obtained is approximately normally distributed. In the case of independence, when H=0.5, the mean and standard deviation of the estimator are functions of sample size n and can be approximated by [13]:

$$\mu = 0.5 - 2.874n^{-0.9067}$$

$$\sigma = 0.7765n^{0.5} - 0.0062$$

Using the above equations, we can evaluate the significance of the estimated Hurst H coefficient.

For bias correction, the estimated Hurst parameter can be substituted in the modified Mann-Kendall variance equation, leading to a V* (S) estimate of the variance of the Mann-Kendall statistic.

However, this variance estimate is a biased estimate of the true V (S) variance when an estimated ETP coefficient from the data is used instead of the true Hurst H coefficient. A bias correction factor B can be obtained to compensate for the sub-estimation of the variance resulting from the H estimation method.

The bias correction factor $\mathbf{B} = \frac{V\,(S)}{V^*\,(S)}$ was obtained from [13] by comparing the theoretical variance with the variance estimated on the basis of a large number of simulated data. The bias correction factor B was regressed on the size n and the coefficient H on the basis of 90,000 simulations of combinations of n = 20 to 200 and H = 0.01 to 0.99. The relationship below leads to a good fit (R^2 = 0.9996):

$$B = a_0 + a_1 H + a_2 H^2 + a_3 H^3 + a_4 H^4$$

Where:

$$a_0 = \frac{1.0024n - 2.5681}{n + 18.6693};\ a_1 = \frac{-2.2510n + 157.2075}{n + 9.2245};\ a_2 = \frac{15.3402n - 188.6140}{n + 5.8917};\ a_3 = \frac{-31.4258n + 549.8599}{n - 1.1040}$$

$$a_4 = \frac{20.7988n - 419.0402}{n - 1.9248}$$

2.3.2 DETECTION OF SINGLE AND MULTIPLE BREAKS

2.3.2.1 KRUSAL WALLIS TEST

The Krusal Wallis test is a non-parametric statistical test used to determine whether data from one period are significantly different from another. It is a test for detecting multiple breaks. It is applied to chronicles whose data have a non-normal distribution and at least 10 values. If the *p*-value of the test is less than the risk of error (5%), there is a difference between the data for at least two periods. The null hypothesis is that the periods are not different from each other. The calculated statistic is defined as follows:

$$K = (n-1)\frac{\sum_{i=1}^{g} n_i\,(\bar{r_i} - \bar{r})^2}{\sum_{i=1}^{g}\sum_{j=1}^{n_i}\,(r_{ij} - \bar{r})^2}$$

Where g is the number of periods, ni is the number of observations in period i, rij is the rank of observation j in the group

i, n is the total number of data, $\bar{r}_i = \frac{\sum_{j=1}^{ni} r_{ij}}{ni}$ and $\bar{r} = \frac{1}{2(n+1)}$.

The statistic is then compared to the quantiles of a Chi 2 distribution with (g-1) degrees of freedom.

2.3.2.2 CUMULATIVE DEVIATION

The Cumulative Deviation is a parametric statistical test used to test whether the means of two parts of a time series are significantly different (for an unknown date of change). It is a test for detecting simple breaks. Its principle is to detect a change in the series mean after m observations:

$$E(x_i) = \mu \quad i = 1, 2, 3, ..., m$$

$$E(x_i) = \mu + \Delta \quad i = m + 1, m + 2, ..., n$$

Where μ is the mean of the data prior to the change and Δ is the change in the mean.

From the averages, the cumulative deviations are calculated as follows:

$S0* = 0 \; S0* = \sum_{i=1}^{k} (x_i - \bar{x}) \quad k = 1, 2, 3, ..., n$

And the recalculated adjusted partial sums are obtained by dividing the Sk * values by the standard deviation:

$$S_k^{**} = S_k^{*} / D_x$$

$$D_x^2 = \sum_{i=1}^{n} \frac{(x_i - \bar{x})^2}{n}$$

The statistical test Q is:: $Q = \max |s_k^{**}|$

It is calculated for each year, with the maximum value indicating the point of change. The critical values of Q/√ (n) are given in Table 1 (see below). A value of S0 * indicates that the mean of the data from the more recent part of the series is significantly higher than that from the older part, and vice versa.

Table 1. Critical value of Q/√ (n) for the cumulative deviation test

N	Q/√ (n) at the level of confidence		
	α = 0.10	α = 0.05	α = 0.01
10	1.05	1.14	1.29
20	1.1	1.22	1.42
30	1.12	1.24	1.46
40	1.13	1.26	1.5
50	1.14	1.27	1.52
100	1.17	1.29	1.55
∞	1.22	1.36	1.63

2.3.3 SPATIAL AUTOCORRELATION WITH THE MORAN INDEX

Spatial autocorrelation is the covariation of properties within geographic space: characteristics at proximal locations appear to be correlated, either positively or negatively [23]. It is an inferential statistic, which means that the results of the analysis are always interpreted in the context of its null hypothesis. It indicates a functional relationship between what happens between a spatial unit and its neighbours [24], [25] proposed a statistic (Moran I) to assess spatial autocorrelation by characterising the correlation between spatially proximate locations, which is defined as:

$$I = \frac{n}{\sum_{i=1}^{n}\sum_{j=1}^{n} W_{ij}} \frac{\sum_{i=1}^{n}\sum_{j=1}^{n} W_{ij} (P_i - \bar{P})(P_j - \bar{P})}{\sum_{i=1}^{n}\sum_{i}} (P_i - \bar{P})^2$$

The Moran index is interpreted according to the following hypothesis:

H0: Neighbours do not co-vary in any particular way.

Iw > 0 => positive spatial autocorrelation

When the P_value returned by this tool is statistically significant, the null hypothesis H0 is rejected.

In the equation (Pi, Pj are rainfall at the i th, j th gauge, respectively, in mm; W ij specified in equation 3 is an element of a spatial weight matrix:

$$W = \frac{W^*}{W_0} = \begin{bmatrix} W_{11} & W_{12\ldots} & W_{n1} \\ W_{21} & W_{21\cdots} & W_{2n} \\ \vdots & \vdots & \ddots & \vdots \\ W_{n1} & W_{n2} & W_{nn} \end{bmatrix}$$

The weight matrix W is derived by normalising the adjacency matrix $W^* = [W_{ij}^*]$ with a normalization factor $W_0 = \sum_{i=0}^{n} \sum_{j=0}^{n} W_{ij}^*$. The values of the matrix W_{ij}^* can be calculated in several ways and are defined at the origin as W_{ij}^* = 1 if i th and j th are adjacent, and W_{ij}^* = 0 otherwise, most commonly. Since 0/1 weighting is used for discrete rather than continuous and geographic data, W_{ij}^* is calculated by the inverse distance method in this study, which is defined as follows:

$$W_{ij}^* = r_{ij}^{-b}$$

Where rij is the distance between the i th template and the j th template, in m; b is a distance parameter (b = 1 in this study).

Moran's I-index formula produces a value for the spatial correlation at proximal locations, i.e. the rainfall measurements in this study, that varies from -1 to 1 [26]. A zero value means a random spatial pattern, and negative values indicate a dispersed spatial distribution while positive values demonstrate correlated spatial features. The Moran Index (MI) close to 1 indicates that there is a high level of positive spatial autocorrelation, and this can be explained by the fact that high/low values are colocated with high/low values [27].

3 RESULTS ET DISCUSSION

3.1 LONG-TERM TRENDS IN ANNUAL RAINFALL

Tables II and III show the results of the classical (MK1), modified (MK2) Mann Kendall (MK1) and modified Mann Kendall (MK2) tests, respectively, on the annual rainfall series for the period 1950-2020. Analysis of long-term rainfall trends at local and catchment scales using the MK1 and MK2 statistical tests revealed significant changes.

If the Hurst effect (H) is not taken into account in the rainfall series, 58% of them show significant downward trends at a 5% risk. 42% of them show downward trends but are not significant at a 5% risk. These results reflect a general decrease in the amount of annual rainfall recorded in the Bandama river catchment. According to [28], [29], [10], this decrease may be a consequence of global warming. Many authors have used different methods to analyse climate variability in other catchment areas in the sub-region, including [30], [31] and [32]. These authors worked on the Bandama Blanc, Comoé, Sassandra and Cavally catchments respectively, and came to the same conclusion, namely that there has been a general decline in rainfall. Taking the Hurst effect into account reduced the number of stations showing significant trends from 58% to 32% at a 5% risk. This result shows that the presence of autocorrelation leads to aberrant trends that are not due to climate change, as indicated by several authors ([33], [13], [34], [35]). En effet, la présence positive ou négative d'autocorrélation biaise la significativité des tests et donc peut conduire à des tendances aberrantes. The positive or negative presence of autocorrelation biases the significance of the tests and can therefore lead to aberrant trends.

Table 2. Characteristics of MK1 and MK2 statistical tests in annual rainfall series from 1950 to 2020 at the local scale

Rainfall station	MK1		Hurst significance (H)		MK2	
	Statistics	*p_value*	value of H	P_value	Statistic	*p_value*
Dabakala	-2.55	**0.005**	0.548	0.207	-0.225	0.057
Boundiali	-3.17	**0.001**	0.631	**0.025**	-0.266	0.082
Korhogo	-2.65	**0.004**	0.466	0.774	-0.23	**0.011**
Ouellé	1.6	0.111	0.480	0.623	0.135	0.188
Oumé	-2.41	**0.008**	0.595	0.069	-0.212	0.121
Séguéla	-1.04	0.189	0.611	**0.045**	-0.105	0.464
Zuénoula	-1.92	**0.03**	0.57	0.129	-0.174	0.171
Béoumi	-2.08	**0.002**	0.488	0.578	-0.247	**0.012**
Tiassalé	-1.87	**0.035**	0.568	0.134	-0.169	0.18
Ouangolodougou	-1.19	0.144	0.664	**0.008**	-0.117	0.489
Niakaramadougou	-1.37	0.1	0.416	0.763	-0.132	0.089
M'Bahiakro	-1.68	0.053	0.400	0.625	-0.155	**0.034**
Mankono	-2.41	**0.008**	0.402	0.643	-0.211	**0.004**
Katiola	-1.79	**0.043**	0.533	0.277	-0.162	0.153
Grd_Lahou	-2.79	**0.003**	0.487	0.587	-0.237	**0.015**
Yamoussoukro	-0.13	0.641	0.277	0.052	-0.038	0.824
Bouake	-1.51	0.073	0.512	0.407	-0.143	**0.003**
Dimbokro	-0.19	**0.02**	0.569	0.133	-0.108	0.139
Bouaflé	-0.038	0.641	0.661	**0.009**	-0.187	0.824

Values of P_value in bold indicate a significant trend at the 5% level; a negative value of the test statistic indicates a downward trend and a positive value indicates an upward trend

Table 3. Characteristics of MK1 and MK2 statistical tests in annual rainfall series from 1950 to 2020 at the watershed scale

Sub-catchment (outlet)	MK1		Hurst significance (H)		MK2	
	Statistics	*p-value*	Value of H	P_value	Statistics	P_value
N'Zi (N'Zianoa)	-0.097	0.234	0.453	0.882	-0.097	0.277
Marahoué (Bouaflé)	-0.245	**0.003**	0.532	0.286	-0.245	**0.032**
White Bandama (Tortiya)	-0.279	**0.001**	0.488	0.579	-0.279	**0.005**
Bandama (Tiassalé)	-0.23	**0.005**	0.496	0.511	-0.237	**0.017**

Values of P_value in bold indicate a significant trend at the 5% level; a negative value of the test statistic indicates a downward trend and a positive value indicates an upward trend

3.2 MULTIPLE AND SINGLE BREAKS

Tables IV and V show, respectively, the results of applying break tests (Cumulative Deviation and Krusal_Wallis) to the rainfall series of nineteen (19) stations over the period 1950-2020. Analysis of the breaks detected shows that, on average, 66% of the rainfall stations predict significant downward breaks at the 5% threshold, with the majority of break years fluctuating around 1970. All of the years of disruption occur during the period of drastic drought (1968-1990) experienced by West Africa. These results are in line with the various points of change detected in several previous studies of climate variability in West Africa ([28], [36]).

The rainfall deficits recorded range from -4% to -24%, which would mean that the various stations successively experienced a wet climatic phase before the disruption and a dry one afterwards. In their studies of points of change and recent rainfall trends in the Cavally basin, the authors [32] concur. In their studies, these authors found two climatic periods separated by a break during the transition from one phase to another. The first phase is wet and generally runs from 1980 to 1995, while the second is dry and runs from 1996 to 2016, with 1996 as the break year.

Using the Cumulative Deviation statistical test, breaks were detected at 68% of the rainfall stations, whereas using the Krusal Wallis statistical test, breaks were detected at just 63% of the rainfall stations. The difference in proportions between

the two tests could be due to the high power of parametric tests compared with non-parametric tests. This assertion is shared by [37], who states in one of his hypotheses that for significance levels of 95% and 90%, the cumulative deviation test (non-parametric test) appears to be more powerful than the Worsley test (parametric test). 63% of the rainfall stations showed significant breaks and 37% showed non-significant breaks at the 5% risk from the two tests used. These breaks mark a change in the rainfall pattern that began in the 1970s. They also confirm the overall decline in rainfall data series around the 1970s. These results corroborate the work of numerous authors in the West African sub-region, namely [9], [4], [38] and in particular in Côte d'Ivoire [29]; [10]; [39] who found breaks around the 1970s in the rainfall series cited by [39].

Table 4. Characteristics of the change point tests from the cumulative deviation of annual rainfall amounts over the period 1950 - 2020

Rainfall station	Years of break-up	Significance index (%)	Deficit
Dabakala	1971	**99.78**	-3,83
Boundiali	1975	**99.99**	-21,71
Korhogo	1970	**99.58**	-16,13
Ouellé	1965	**98.26**	**25,54**
Oumé	1979	**99.84**	-15,25
Séguéla	1979	89.7	-17,95
Zuénoula	1971	**99.62**	-17,25
Béoumi	1966	**99.62**	-18,04
Tiassalé	1969	**99.72**	-16,54
Ouangolodougou	1970	94.31	-12,37
Niakaramadougou	1968	85.41	-10,51
M'Bahiakro	1974	**95.95**	-11,50
Mankono	1971	**97.32**	-13,32
Katiola	1980	**97.7**	-14,87
Grand Lahou	1971	**99.94**	-23,63
Bouake	1972	72.77	-8,01
Dimbokro	1968	80.25	-6,26
Bouaflé	1972	**99.26**	-17,09
Yamoussoukro	2000	93.47	**10,38**

Significance values in bold indicate a point of change with a 5% risk of error

Table 5. Characteristics of the change point tests from Krusal_Wallis of annual rainfall amounts over the period 1950 – 2020

Rainfall station	Homogeneous periods	Significance index (%)	Deficit
Dabakala		**99.8**	-3,83
Boundiali		**95.41**	-21,71
Korhogo		**99.42**	-16,13
Ouellé		82.8	**25,54**
Oumé		**95.98**	-15,25
Séguéla		**96.54**	-17,95
Zuénoula		**99.31**	-17,25
Béoumi		**98.73**	-18,04
Tiassalé	1950 -1970; 1971-1990	**99.81**	-16,54
Ouangolodougou		94.46	-12,37
Niakaramadougou		72.13	-10,51
M'Bahiakro		80.81	-11,50
Mankono		**96.26**	-13,32
Katiola		93.46	-14,87
Grand Lahou		**99.81**	-23,63
Bouake		68.95	-8,01
Dimbokro		62.67	-6,26
Bouaflé		**98.99**	-17,09
Yamoussoukro		**99.55**	**10,38**

Significance values in bold indicate a point of change with a 5% risk of error

3.3 AUTOCORRÉLATION SPATIALE DES PLUIES ANNUELLES

Table VI shows the spatial autocorrelation of the nineteen rainfall stations using Moran's statistical test. The results show that there is a statistically significant spatial autocorrelation at the 5% threshold within the annual rainfall series of the different stations. The positive value of the Moran index (0.232) indicates that the spatial distribution of high and low values in the rainfall series has been subject to greater spatial aggregation, i.e. high values are aggregated with other high values and low values with other low values [27]. This could either be due to the fact that the stations are subject to practically the same climatic effects or hazards or it could also be due to the values of certain stations being spatially autocorrelated [40].

Table 6. Characteristics of the Moran statistical test of rainfall data

Variables	IM	Z-Score	p_value	Interpretation of Moran Index (MI)
Rain	0.232	1.94	0.053	Positive spatial autocorrelation

Values of P_value in bold indicate a significant trend at the 5% level

4 CONCLUSION

This study was carried out with the aim of understanding long-term rainfall trends in the Bandama river catchment. The study showed that failure to take account of the Hurst effect in the rainfall series can modify the trend results. The year 1970 appears to be the year of the rainfall disruption in the catchment, with deficits ranging from 6% to 23%. The study also revealed a positive spatial correlation between the rainfall stations in the catchment.

REFERENCES

[1] GIEC, Changements Climatiques: Rapport de synthèse, 2014.

[2] Hubert P., CarbonneL J.P. et CHAOUCHE A. (1989). Segmentation des séries hydrométéorologiques. Application à des séries de précipitations et de débits de l'Afrique de l'Ouest. Journal of Hydrology, vol. 110, n° 3-4, pp. 349-367. DOI: 10.1016/0022-1694 (89) 90197-2.

[3] Bricquet J.P., Bamba F., Mahe G., Toure M. et Olivry J.C. (1997). Variabilité des ressources en eau de l'Afrique Atlantique, PHI-V, 6, pp. 83-95.

[4] Servat E., Paturel J.-E., Lubes-Niel H., Kouame B., Masson J.M., Travaglio M. et Marieu B. (1999). De différents aspects de la variabilité de la pluviométrieen Afrique de l'ouest et centrale non sahélienne, Revue des sciences de l'eau, 12, 2, pp. 363-387.

[5] Brou T., Servat E. et Paturel J.E., 1998, Activités humaines et variabilité climatique: cas du sud forestier ivoirien, IAHS, 252, pp. 365-373.

[6] Kouassi A.M., Kouame K.F., Saley M. B., & Biemi J. (2013). Impacts des changements climatiques sur les eaux souterraines des aquifères de socle cristallin et cristallophyllien en Afrique de l'Ouest: cas du bassin versant du N'Zi-Bandama (Côte d'Ivoire). Larhyss Journal, N°16, pp. 121-138.

[7] Aka A.A., Lubès H., Masson J.M., Servat., Paturel J.E. & Kouamé B. (1996). Analyse de la variabilité temporelle des écoulements en Côte d'Ivoire: approche statistique et caractérisation des phénomènes. Journal des Sciences Hydrologiques, vol. 41, n° 6, pp. 959-970.

[8] Mahé G et Olivry J.C. (1995). Variations des précipitations et des écoulements en Afrique de l'Ouest et centrale de 1951 à 1989. Sécheresse, vol. 6, n° 1, pp. 109-117.

[9] Paturel J.E., Servat E. & Delattre M.O. (1998). Analyse de séries pluviométriques de longue durée en Afrique de l'Ouest et centrale non sahélienne dans un contexte de variabilité climatique. Journal des Sciences Hydrologiques, vol. 43, n° 6, pp. 937-945.

[10] Goula B.T.A., Savané I., Konan B., Fadika V. et Kouadio B.G. (2006). Impact de la variabilité climatique sur les ressources hydriques des bassins de N'zo et N'zi en Côte d'Ivoire (Afrique tropicale humide). VertigO, vol. 7, n° 1, pp. 1-12.

[11] Kanohin F., Saley M.B. et Savané I. (2009). Impacts de la variabilité climatique sur les ressources en eau et les activités humaines en zone tropicale humide: cas de la région de Daoukro en Côte d'Ivoire. European Journal of Scientific Research, vol. 26, n° 2, pp. 209-222.

[12] Kouakou K. E., Goula B.T.A. and Savané I. Impacts of climate variability on surface water resources in the humid tropics: the case of the trans boundary Comoé basin (Côte d'Ivoire-Burkina Faso). European Journal of Scientific Research, vol. 16, no. 1, 2007. pp. 31-43.

[13] Hamed K. H., 2008. Trend detection in hydrologic data: The Mann-Kendall trend test under the scaling hypothesis, Journal of Hydrology, 349: 350-363. http://dx.doi.org/10.1016/j.jhydrol.2007.11.009

[14] Mann (1945) Mann HB. (1945). Nonparametric tests against trend, Econometrica; 13: 245–59. McGilchrist CA, Woodyer KD, Note on a distribution-free CUSUM technique, Technometrics 1975; 17 (3): 321–5.

[15] Kendall (1975) Kendall MG. (1975). Rank correlation methods, p. 202., Griffin, London.

[16] Hirsch, R. M. & Slack, J. R. (1984). Un test de tendance non paramétrique pour les données saisonnières avec dépendance série. Recherche sur les ressources en eau/ Volume 20, Numéro 6 / pp. 727 - 732.

[17] Dennis Helsel & Hirsch. Statistical Methods in water resources. Elsevier, 1992.

[18] Helsel & Hirsch (2002) Helsel DR., Hirsch RM. Statistical Methods in Water Resources Techniques of Water Resources Investigations, Livre 4, Chapitre A3. Enquête géologique des États-Unis. 522 pages. 2002.

[19] Hamed KH., Rao R. A modified Mann-Kendall trend test for autocorrelated data. J. Hydrol. 1998; 204, pp. 182-196.

[20] Lopez B., Leynet A., Blum A, Baran N. (2011). Evaluation des tendances d'évolution des concentrations en polluant dans les eaux souterraines: Revue des méthodes statistiques existantes et recommandations pour la mise en place de la DCE. Rapport final BRGM/RP-59515-FR. 2011.

[21] Mcleod & Hipel (1978). Préservation de la plage ajustée rééchelonnée: 1. une réévaluation du phénomène de Hurst. https://doi.org/10.1029/WR014i003p00491.

[22] Sen P. K. (1968). Estimations du coefficient de régression basées sur le Tau de Kendall, *Journal of the American Statistical Associatio*n, 63: 324, pp 1379 - 1389, DOI: 10.1080/01621459.1968.10480934.

[23] Legendre (1993). Autocorrélation spatiale: problème ou nouveau paradigme? Ecologie / Tome 74, Numéro 6 / pp 1659 - 1673. https://doi.org/10.2307/1939924.

[24] Papa Ousmane Cisse (2018). Etude de modèles spatiaux et spatio-temporelles. Topologie algébrique [math.AT]. Université Panthéon-Sorbonne - Paris I; Université de Saint-Louis (Sénégal), Français. NNT: 2018PA01E060. tel-02065990.

[25] Moran P. (1950). Notes on continuous Stochastic Phenomena. Biometrika, pp. 17 - 23.

[26] Stephens, EM; Bates, PD; Freer, JE; Mason, DC. (2012). L'impact de l'incertitude des données satellitaires sur l'évaluation des modèles d'inondation. J. Hydrol, 414, pp. 162 - 173.

[27] Tiefelsdorf M. (1998). Quelques applications pratiques de la distribution conditionnelle exacte de Moran I. Articles en sciences régionales 77 (2), pp. 101 - 129.

[28] Assemian, E. A., Kouame, F. K., Djagoua, E. V., Affian, K., Jourda, J., Adja, M., Lasm, T. & Biemi, J. (2013). Etude de l'impact des variabilités climatiques sur les ressources hydriques d'un milieu tropical humide: cas du département de Bongouanou (Est de la Côte d'Ivoire). Revue des sciences de l'eau / Journal of water science, 26 (3), pp. 247 - 261. https://doi.org/10.7202/1018789ar.

[29] Savané I., Coulibaly K. et Gioan P. (2001). Variabilité climatique et ressources en eau souterraine dans la région semi-montagneuse de Man. Sécheresse, 12 (4), pp. 231 - 237.

[30] Kouakou, K. E. (2011). Impacts de la variabilité climatique et du changement sur les ressources en eau en Afrique de l'Ouest: Cas du bassin versant de la Comoé. Thèse unique de doctorat, Université d'Abobo-Adjamé, 170 p.

[31] Kouakou (2019). Impact des Evolutions Climatiques sur les Ressources en eau des Petits Bassins en Afrique Sub-Saharienne: Application au Bassin Versant du Bandama à Tortiya (Nord Côte d'Ivoire). European Scientific Journal March Édition Vol.15, No.9 ISSN: 1857 - 7881 (Print) e - ISSN 1857 – 7431.

[32] Yao & Soro (2021a). Tendance récente des précipitations et changements brusques sur le bassin versant du Cavally (Afrique de l'Ouest).Journal international de l'environnement et du changement climatique, 11 (12). pp. 52 - 66. ISSN 2581 – 8627.

[33] Soro G. E., Goula B. T. A., Kouassi F. W. & Srohourou B. (2010). Evolution des intensités maximales annuelles des pluies horaires en Côte d'Ivoire. Agronomie Africaine, 22 (1): pp 33 - 44.

[34] Biteye (2009). Evolutions dans les régimes Hydrologiques extrêmes en France: changement climatique et phénomène de Hurst. Sciences de l'environnement.

[35] Yao & Soro, 2021a et b. Detection of Hydrologic Trends and Variability in Transboundary Cavally Basin (West Africa). American Journal of Water Resources, 2021, Vol. 9, No. 2, pp. 92-102.
Available online at http://pubs.sciepub.com/ajwr/9/2/6 + Published by Science and Education Publishing DOI: 10.12691.

[36] Doumouya I., Kamagaté B., Bamba A., Ouédraogo M., Ouattara I., Savané I., Goula B. T. A., Biemi J. (2009). Impact de la variabilité climatique sur les ressources en eau et végétation du bassin versant du Bandama en milieu intertropical (Côte d'Ivoire). Rev. Ivoir. Sco. Technol., 14 (2009).pp 203 - 215 ISSN 1813 - 3290.

[37] Soro G, E., (2011). Modélisation statistique des pluies extrêmes en Côte d'Ivoire, Thèse Doctorat d'Etat de l'Université Nangui Abrogoua Abidjan, pp. 39-43.

[38] Ardoin B.S. (2004). Variabilité hydroclimatiques et impacts sur les ressources en eau de grands bassins hydrographiques en zone soudano-sahélienne, Thèse de Doctorat, Université de Montpellier II, France, 330 p.

[39] Kouassi A.M., Kouamé K.F., Goula B.T.A., Lasm T., Paturel J.E. & Bmi J. (2008). « Influence de la variabilité climatique et de la modification de l'occupation du sol sur la relation pluie-débit à partir d'une modélisation globale du bassin versant du N'Zi (Bandama) en Côte d'Ivoire«, Revue Ivoirienne des Sciences et Technologie, vol. 11, pp 207-229.

[40] Gallo J. L. (2002). Économétrie spatiale: l'autocorrélation spatiale dans les modèles de régressions linéaire. Dans Economie & Prévision 2002/4 (n°155), pp 139 - 157.